

Effect of Dimples/Protrusion Concavity on Heat Transfer Performance of Rotating Channel

Cong-Truong Dinh*, Minh-Sang Le, Khanh-Duy Cong Do, Duy-Hung Chung
School of Mechanical Engineering, Hanoi University of Science and Technology, Ha Noi, Vietnam
*Corresponding author email: truong.dinhcong@hust.edu.vn

Abstract

The continuing increase in gas turbine inlet temperature requires additional heat transfer at the trailing edge. Therefore, a large amount of research has been carried out to find a highly efficient cooling process for gas turbine blades. Pin-fins have been widely used in the trailing edge of gas turbines to enhance heat transfer performance. Pin-fins also strengthen the structure between the inlet and outlet faces of the gas turbine. According to previous research, the flow structure and heat transfer characteristics are influenced by many parameters of the pin-fin array, especially the pin-fin shape, height, diameter as well as layout. In this study, instead of changing the structure of the pin-fin array, the work focused on the design of protrusion/dimple points on the leading and trailing edges. Numerical simulations using the SST (Shear Stress Transport) turbulence model were performed to investigate the effect of dimple/protrusion concavity on flow structure and heat transfer characteristics in a rotating channel with pin-fin array. The pin-fins are arranged staggered to each other. The results show that when changing the dimple/protrusion concavity on the leading and trailing edges combined with the rotation speed, the heat transfer efficiency changes positively.

Keywords: Pin-fin array, dimple, protrusion, RANS, Nusselt number.

1. Introduction

In aircraft engines, turbines are an indispensable part that converts the energy of the gas flow after the combustion chamber into mechanical energy to drive other parts. Turbine blades are in constant contact with hot air, so cooling is always the most interesting field in turbine research. There are many cooling techniques in turbine blades, the most common of which are internal cooling and external film cooling. Internal cooling includes convection cooling, turbulent ribs cooling, and pin-fins cooling. In the pin-fin array structure, the pin-fins are arranged and used at the trailing edge of the turbine blade both to increase heat transfer capacity, reduce the temperature at the outlet as well as increase the rigidity of the structure. In order to improve the heat transfer capacity of the turbine blade outlet and limit the pressure loss of the cooling stream, it is important to study the shape and arrangement of the pin-fin array. Pin-fin arrays act like turbulators to disrupt the laminar flow and increase disturbances in the channel due to the separation of the flow as it passes through the pin-fins. This reduces the corresponding cross-section to an increase in momentum and heat transfer capacity.

Over the years, a large number of studies have been carried out to find the best parameters of the pin-fin array to enhance heat transfer with as little stress as possible. Li *et al.* [1] used the naphthalene sublimation technique to investigate the heat transfer properties in rectangular channels with elliptical pin-fin arrays. This

study shows that the elliptical pin-fins have better thermal efficiency than the round pin-fin. Hwang *et al.* [2] investigated the effect of pin-fin array geometry (square, rhombus, and circle) on heat transfer in a 90 degree rotating channel. It was found that the square pin-fins had the highest Nusselt number compared to other cases. Xu *et al.* [3] also studied the effect of pin-fin array shape on heat transfer in a rectangular channel. Six different shapes (circle, ellipse, rhombus, teardrop, NACA, and L-shape) were investigated experimentally. The results show that round Pin-fins have the highest Nusselt number compared to other cases.

The most common factors to investigate while studying pin-fins are heat transfer and pressure drop. It is essential to clearly understand the mechanism that governs these factors of pin-fin channel. Pin-fin arrays act like turbulators to disrupt the laminar flow and increase turbulence in the rectangular channel due to the separation of the flow as it passes through the pins. This reduces the corresponding cross-section by increasing momentum and heat transfer capacity. Sparrow *et al.* [4] experimentally studied the heat transfer of in-line and staggered pin-fin arrays installed in the internal cooling channel. They concluded that the staggered pin-fin arrays significantly increase the heat transfer across the turbine blade, but the pressure drop is also higher. Chyu [5] explored the influence of the staggered short pin-fin arrays with endwall fillet and the effect when using mass transfer coefficient Sh

through vaporization naphthalene on the heat transfer capacity and pressure drop by experimental tests. Their results showed that the pin-fin arrays with endwall fillet show lower mass transfer coefficient, mass transfer rate, performance index, and higher pressure drop than the normal form. However, as the Reynolds number increases, this effect is minimized. In summary, the endwall fillet is found to be undesirable for improving heat transfer efficiency.

To enhance the heat transfer capacity of the turbine trailing edge while minimizing the pressure drop across the heated channel, the research of pin-fin arrays configurations has become more and more remarkable. Ostanek and Thole [6] while measuring the time-dependent near wake flow and the local heat transfer coefficients in several pin-fins channels with the individual variation of the height-to-diameter ratio (H/D), the spanwise spacing-to-diameter ratio (S/D), and the streamwise spacing-to-diameter ratio (X/D), found that H/D has little effect on the wall-normal gradient through the middle portion of the duct, reducing S/D can limit vortex generation in the first row.

In addition to the shape of the pin-fins, its height-to-diameter ratio also has a great influence on heat transfer. The effect of the height-to-diameter ratio on heat transfer was investigated by Chyu *et al.* [7]. The experimental results show that the Nusselt number and coefficient of friction are higher with a lower height-to-diameter ratio while it is lower with a higher height-to-diameter ratio. However, the cooling structure faces a challenge due to the increasing inlet temperature of the gas turbine. Therefore, a large amount of research has been carried out to find a highly efficient cooling

structure for gas turbines. Creating dimple/protrusion on the inlet and trailing edges is a new technology.

Many researchers have incorporated a protrusion/dimple pin-fin array to enhance heat transfer at the trailing edge of the gas turbine. Rao *et al.* [8-10] used protrusion/dimple in a rectangular channel with pin-fins. It was found that the application of the protrusion/dimple increased the Nusselt number in a pin-fin array channel. Luo *et al.* [11] also combine the protrusion/dimple with the pin-fin array on the posterior edge. However, the channel of the trailing edge is a wedge channel and not a rectangular channel. The results show that the position and height of the protrusion/dimple have a great influence on the heat transfer capacity of the channel. Experimental studies are almost done on fixed channels. According to previous studies, it was found that rotation has a significant effect on the flow structure and heat transfer both in the dimple channel and the pin-fin channel. However, few papers have been published on the flow structure and heat transfer on the rotating channel with dimple/protrusion combined with pin-fin array. Therefore, heat transfer and flow structure in pin-fin channel with different dimple/protrusion heights were investigated in this study.

2. Numerical Analysis

2.1. Design Description

Fig. 1 shows a diagram of the pin-fin array channel with different concavity of dimples/protrusion in this study. This is a rectangular channel with height $H = 19.05$ mm and width $W = 15.875$ mm. The hydraulic diameter of the channel is $D_h = 2HW/(H+W)$, is 18.96 mm.

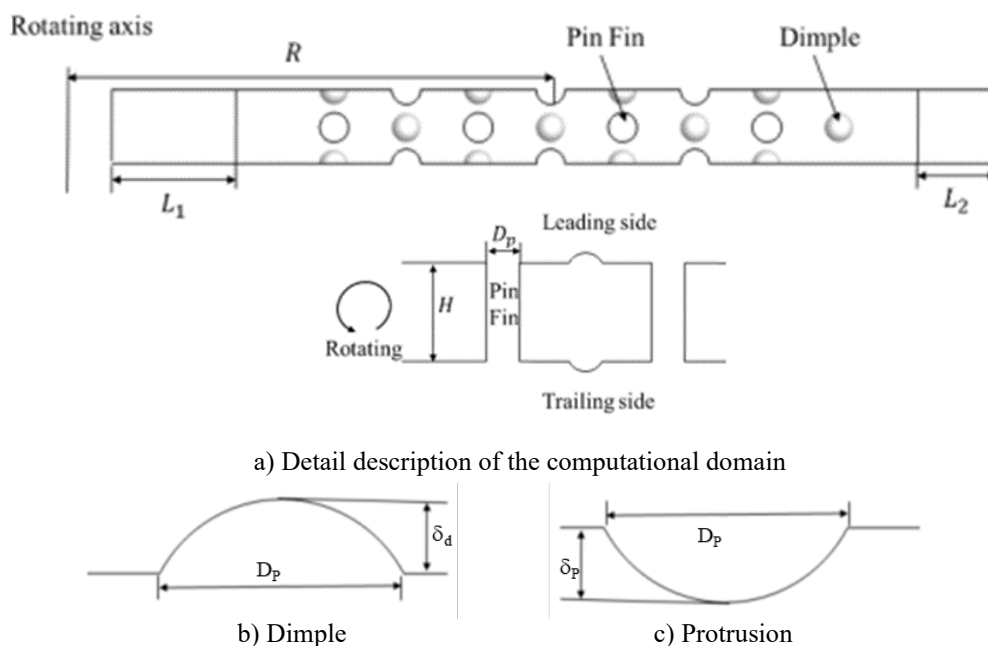


Fig. 1. Schematic computational domain and dimple, protrusion shapes.

Table 1. Geometric variations for dimples and protrusions

Cases	Arrangement	δ/D_d
Baseline	--	0
Case 1	Dimple	0.1
Case 2	Dimple	0.4
Case 3	Protrusion	0.1
Case 4	Protrusion	0.4

Inlet channel length of $L_1 = 150$ mm and $L_2 = 100$ mm. Pin-fin has a diameter of $D_p = 6.35$ mm. Pin-fin is staggered with streamwise distance of $S_2 = 15.875$ mm and spanwise distance of $S_1 = 15.875$ mm. All dimples/protrusions are put between the pin-fins. The diameter of the protrusion/dimple part is $D_d = D_p = D$. In order to investigate the influence of dimples/protrusions on flow structure and heat transfer under rotational conditions, five different dimples/protrusions were investigated in this study as $\delta/D_d = 0, 0.1, 0.2, 0.3, 0.4$ as shown in Table 1. The turning radius is $R = 420$ mm.

2.2. Numerical Method

Commercial software ANSYS CFX 19.1 [12] with the $k-\omega$ SST turbulence model was used in this work to study the flow and heat transfer characteristics in the main channel. For the meshing, in this study, the mesh was generated using ICEM from Ansys 19.1 to create a mesh system with the lowest mesh quality of 0.65 and the highest of 0.8. This shows that the mesh quality of the channel is quite good. An example of an unstructured grid is shown in Fig. 2. The y^+ value near the wall is approximately 1. In the areas near dimple/protrusion and the pin-fins are divided into O-grid mesh.

The problem runs about 1,000 iterations. Furthermore, temperature control at the heat transfer surfaces, calculated domain-wide averaged temperature, and outlet mass flow rate was monitored to confirm that convergence criteria were achieved. Calculations are performed on a computer with Intel(R) Xeon(R) CPU X5675 @ 3.07 GHz configuration. For each case, the calculation time ranges from 9 to 11 hours depending on the computation volume.

2.3. Boundary Conditions

In this study, incompressible dry air was used as the cooling air. Experimental results [9], which are similar to this study, are used to compare with numerical results. Wall heat flux $Q = 1000$ W/m², constant inlet temperature $T = 300$ °K is set. The outlet pressure is set to an average static pressure of 1atm.

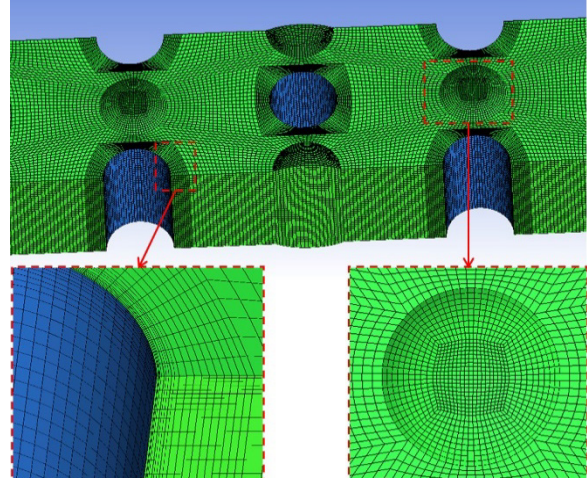


Fig. 2. Grid system example.

The two side boundaries are set as periodic boundary condition. The turbulence intensity is 5%, the viscosity ratio is set to 10, the Reynolds number examined is 7000. The rotating number according to the input speed and hydraulic diameter is 0.2. Convergence criteria are set to that the Root Mean Square (RMS) relative residual values of all flow parameters are lower than 10^{-6} , outlet flow, outlet temperature change lower than 0.03% after 100 loops.

2.4. Parameter Definition

Reynolds number based on the hydraulic diameter of the channel is defined as:

$$Re = \frac{\rho u D_h}{\mu} \quad (1)$$

where μ is the dynamic viscosity.

The convective heat transfer coefficient of the heated surfaces is defined as:

$$h = \frac{q}{T_w - T_b} \quad (2)$$

where q is the heat flux of the heated wall, T_w is wall temperature, T_b is the bulk temperature of the fluid.

The Nusselt number is defined as:

$$Nu = \frac{h D_h}{\lambda} \quad (3)$$

with λ is the thermal conductivity coefficient of air.

According to the correlation formula of Dittus-Boelter [13], the number Nu_0 for the turbulent flow in a smooth channel of a rectangular cross-section is:

$$Nu_0 = 0,023 Re^{0.8} Pr^{0.4} \quad (4)$$

Rotation number:

$$R_0 = \frac{\Omega D_h}{u} \quad (5)$$

with Ω is the rotational speed of the channel.

3. Result and Discussion

3.1. Mesh Dependency and Validation

The smooth pin-fin array channel model is simulated with the $k-\omega$ turbulence model, four types of mesh are selected to choose the most optimal mesh for simulating a dimple/protrusion and pin-fin array channel. The experimental results by Rao *et al.* [9] for Nusselt number ratio of leading and trailing edges are 2.47 and 2.67, respectively. As shown in Fig. 3, the results of the grid test show that grid 1 and grid 2 have a larger Nusselt error than the experimental results when grid 3 and grid 4 give results close to experimental results. Based on the grid graph below, we can see that grid 3 to grid 4 gives not too much deviation, while grid 4 has nearly 1.2 times the number of grids in grid 3. So, grid 3 is considered and is the optimal mesh and is used to perform the simulation.

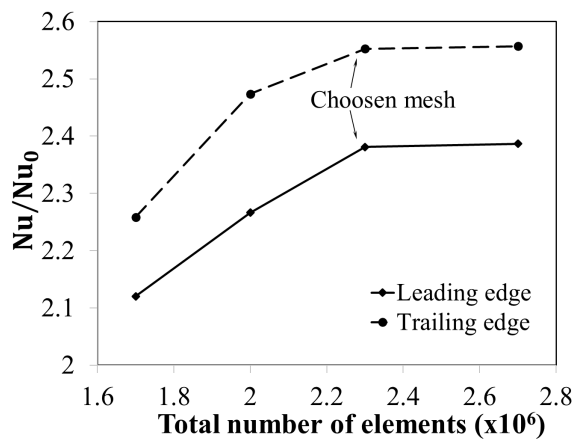
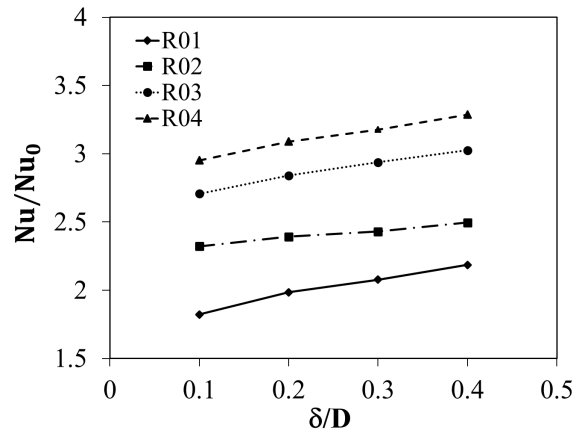


Fig. 3. Mesh convergence.

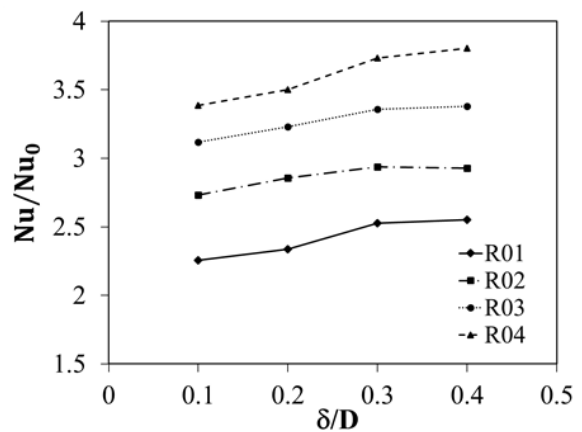
3.2. Effect of Dimple and Protrusion Designs

In this study, while using the verified mesh, simulations for the case of pin-fin array channel with convexity or concavity $\delta/D_a = 0, 0.1, 0.2, 0.3, 0.4$ are performed, the image of the results obtained shows the influence the flow structure and heat transfer in the rotating pin-fin array channel.

From Fig. 4, it can be seen that the indented surfaces show a greater dependence on the rotating number than all the other surfaces, with an almost 100% improvement in the enhancement from the no rotation from lowest to highest. Leading surfaces containing dimples show less dependence on the rotating number than trailing surfaces due to the thick and stable boundary layer on the surface. The small asymmetry between the two leading surfaces is due to experimental uncertainty. The secondary current produced by the dimples does not have a single primary direction and is likely to reduce the intensity of the Coriolis vortices. Thus, the rotation effect is reduced for the side walls of the dimples channel.



a) Leading edge



b) Trailing edge

Fig. 4. The dependency of the Nusselt number on the concavity of the dimples with respect to rotating numbers.

Fig. 5 depicts the comparison of thermal efficiency of pin-fin array channels with different dimple/protrusion depths. In channels containing dimples, the trailing edge has a higher Nusselt number and is about 15% higher than the input edge. Nu/Nu_0 is increased as the concavity of the dimple increases. However, the rate of increase decreases as the dimple concavity increases at the exit edge. Nu/Nu_0 at the leading edge is reduced at a shallow depth (Case 1) compared to the base case. This is because the Nusselt number near Horseshoe Vortex (HV) is reduced in Case 1. When the concavity of the depression is greater than 0.1. Nu/Nu_0 at the leading edge increases because the concavity increases the Nusselt number at the back of the indented surface. Fig. 5 also shows that convexity/dimple has different effects on Nu/Nu_0 . The dimple channel has a higher Nu/Nu_0 at the trailing edge than the protrusion channel. However, the protrusion channel has a higher Nu/Nu_0 at the leading edge than the dimple channel. Due to the Coriolis force, the Nusselt number is low at the front while high at the

rear. The use of a dimple has a significant effect on the flow structure and heat transfer. As the concavity of dimple increases, the velocity near the front decreases slightly while the velocity near the rear decreases significantly. In addition, a low-speed recirculation was found at the top of the dimple. The Nusselt number in the dimple surface is increased both at the front and rear. However, the rear has a higher Nusselt number. The use of a protrusion also has an effect on the flow structure and heat transfer. The HV remains constant at the back and a rotating counter-vortex is observed at the top of the overhang. The Coriolis force causes the opposing vortex to increase at the rear. The Nusselt number near the protrusion is increased as the convexity of the protrusion increases.

The dimple channel behaves similarly to the protrusion channel in terms of the same geometrical and flows parameters as shown in Fig. 6. In the investigated cases, it was found that the protrusion channel has a higher heat transfer enhancement when compared with the dimple channel. This is evident even at the lowest number of rotations, suggesting that although the dimple channel provides less enhancement at some surfaces, it behaves very similarly to the protrusion channel with increasing rotational effects. The increased rotating number leads to an increase in the Nusselt number in all cases. R01, R02, R03 and R04 are the values of Nu/Nu_0 at the different rotation number; 0.1, 0.2, 0.3 and 0.4, respectively.

3.3. Pin-Fin Array Channel with Dimples

Fig. 7 shows the Turbulent Kinetic Energy (TKE) distribution on the tangent plane to the pin-fin array in Case 0, Case 1, and Case 2, the streamlined line near the end wall is curved by the dimple surface. However, the circulation at low speed is not visible inside the dimple. In Case 3 and Case 4, a low-speed cyclic region is found in the dimple. The area of the low-speed circulation area is increased at the input edge while it is decreased at the output edge. This is due to the Coriolis force pushing air toward the trace. On the other hand, the circulation at low speed is increased as the concavity of the dimple increases. Fig. 7 also shows the distribution of TKE on the forward-flow plane. High TKE is found downstream of the pin-fin in case 0. The core region of high TKE is close to the back surface under rotation. It was also found that the TKE increased clearly at the back after applying the dimple. However, the dimple has little effect on the TKE on the side. In addition, TKE is affected by the concavity of the dimple. The TKE near the output edge dimples is increased as its concavity increases. However, it is decreasing in the central part.

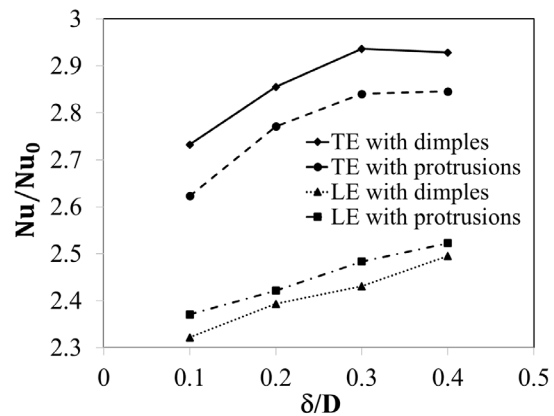
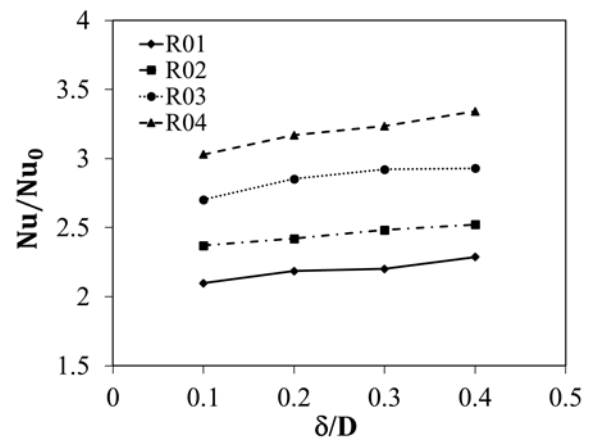
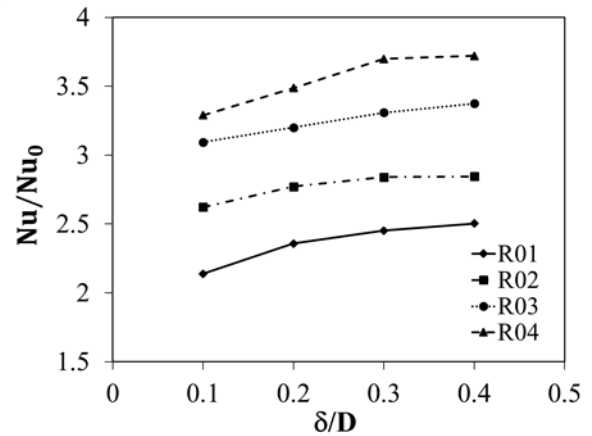


Fig. 5. The dependency of the concavity and convexity on the Nusselt number ratio.



a) Leading edge



b) Trailing edge

Fig. 6. The dependency of the Nusselt number on the convexity of the protrusions with respect to rotating numbers.

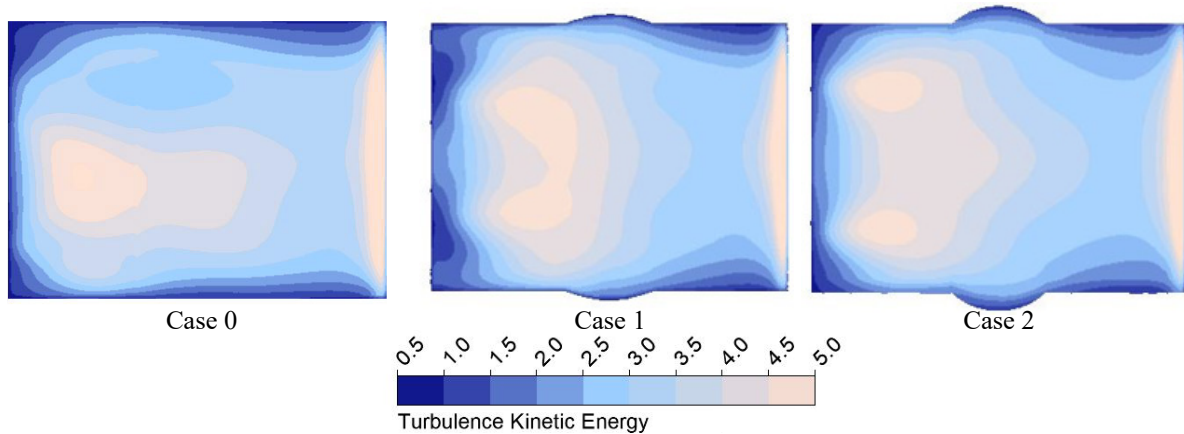


Fig. 7. TKE distributions on the tangent plane to the pin-fin arrays

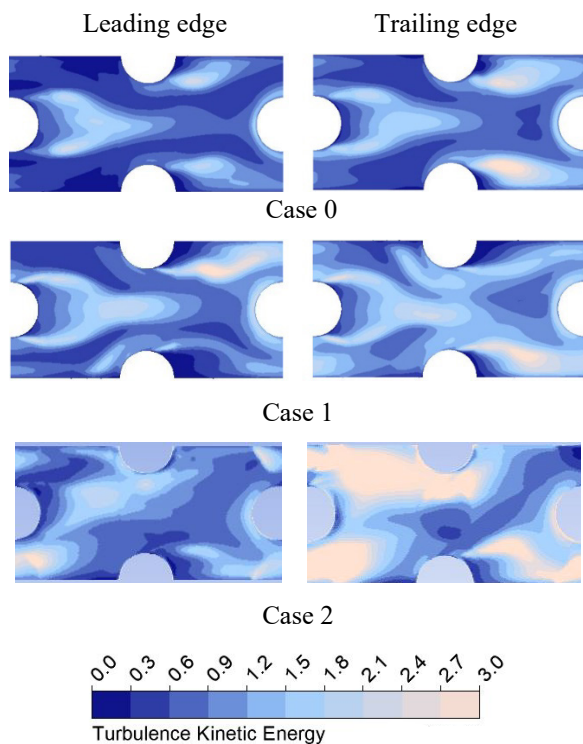


Fig. 8. TKE distributions on planes near leading and trailing edges

Fig. 8 shows a comparison of the TKE distribution near the end wall surface at the leading and trailing edges between Case 0, Case 1, Case 2. It is found that the rotation effect leads to a different TKE distribution characteristic between the leading and trailing edges. In Case 0, the highest TKE was found near HV. This is because HV increases the mix between the main stream and the marginal stream. High TKE is beneficial for enhanced heat transfer on the endwall. The secondary highest TKE is found in front of the pin-fin. This is due to the flow acting on the front face of the pin-fin. The impact effect destroys the nearby boundary layer. Low TKE is observed in

the wake region due to low momentum. Fig. 8 also shows that the rear has a higher TKE than the front side. Further, Fig. 8 shows that the use of dimple increases TKE both at the front and rear. In case 1, it is found that dimples have a small effect on TKE near pin-fins. However, TKE increased slightly in the posterior part of the dimple surface. In Case 2, the TKE at the tip increases slightly as the concavity of the dimple increases. However, it rises sharply posteriorly, especially in the posterior part of the dimple surface and its downstream side. This is because the impact becomes stronger as the concavity of the dimple increases.

3.4. Pin-Fin Channel with Protrusions

Fig. 9 shows a comparison of TKE between Case 3, Case 4. High TKE is found downstream of the pin-fin. TKE decreased as protrusion convexity increased in the mainstream. It was also found that the TKE was increased downstream of the protrusions due to the wake flow produced by the protrusion. However, the TKE in this region is higher at the output edge than at the input edge. High TKE is beneficial for enhanced heat transfer. When the overhang convexity is 0.4, a split bubble is found behind the overhang, i.e. Case 4. The split point moves upstream of the overhang as the protrusion convexity increases.

Fig. 10 shows the comparison of TKE distribution near the wall surface between Case 3 and Case 4. The results show that the TKE distribution is affected by the convexity of protrusions significantly. Case 3 has a shallow convexity, the highest TKE is found between the wake flow and HV regions. TKE has slightly increased anteriorly of the condyle both anteriorly and posteriorly. In addition, the back of the endwall has a higher TKE than the front under the Coriolis force. In case 4, there are many changes in TKE near HV. That is, the Convexity of the overhang has a slight effect on the TKE distribution near the pin-fin.

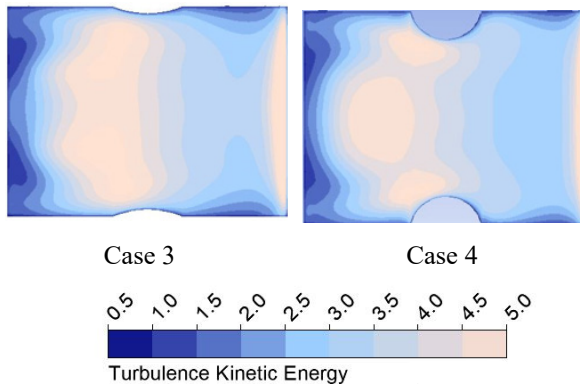


Fig. 9. TKE distribution with cases 3 and 4

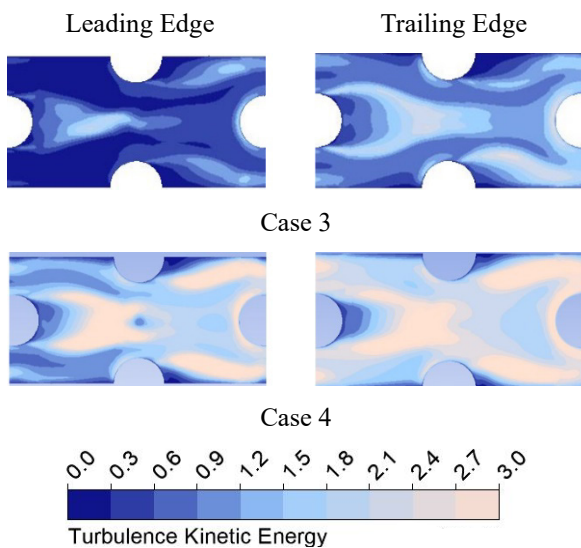


Fig. 10. TKE distributions on planes near leading and trailing edges

However, TKE was increased near the condyle, especially at the anterior aspect of the condyle. This is because obstruction increases turbulence. TKE is also increased downstream of the overhang compared to Case 3. TKE in Case 4 is also increased on the bulkhead surface. This is beneficial for enhancing heat transfer.

4. Conclusion

In this study, a numerical method was performed to investigate the effect of dimple/protrusion depth on flow structure and heat transfer in a rotating channel with pin-fins. The main conclusions can be summarized as follows:

- In a pin-fin array channel with no dimple/protrusion, HV plays an important role in flow structure and heat transfer. High Nusselt number regions are found at the top edges of pin-fins, and low Nusselt numbers are found in the wake flow regions. Due to the Coriolis force, the Nusselt number is low at the leading edge and high at the trailing edge.

- The use of dimples has a significant effect on the flow structure and heat transfer. As the dimple concavity increases, the velocity near the leading edge decreases slightly while the velocity near the trailing edge decreases significantly. In addition, a low-speed recirculation was found at the top of the dimples. The Nusselt number in the dimple surface is increased at both the input and output edges. However, the output edge has a higher Nusselt number.
- The use of overhangs also has an effect on the flow structure and heat transfer. The HV remains constant at the backside and a rotating counter-vortex is observed at the top of the overhang. The Coriolis force causes the opposing vortex to increase at the rear. The Nusselt number near the protrusion is increased as the convexity of the protrusion increases.

More research needs to be conducted to study the effect of changing rotation angle and rotation number and changing the position as well as the diameter of the protrusions along O_x and O_y axes on heat transfer performance of the channel.

Acknowledgments

This study is funded by Hanoi University of Science and Technology (HUST) under grant number T2021-PC-039.

References

- [1] Li, Q., Chen, Z., Flechtner, U., and Warnecke, H. J., Heat transfer and pressure drop characteristics in rectangular channels with elliptic pin fins, *International Journal of Heat and Fluid Flow*, 19(3), 245–250. (1998).
[https://doi.org/10.1016/s0142-727x\(98\)00003-4](https://doi.org/10.1016/s0142-727x(98)00003-4)
- [2] Hwang, J. J., Lu, C. C., Lateral-flow effect on endwall heat transfer and pressure drop in a pin-fin trapezoidal duct of various pin shapes, *Journal of Turbomachinery*, 123(1), 133, (2001).
<https://doi.org/10.1115/1.1333093>.
- [3] Xu, J., Yao, J., Su, P., Lei, J., Wu, J., and Gao, T., Heat transfer and pressure loss characteristics of pin-fins with different shapes in a wide channel, In *Proceedings of the ASME Turbo Expo (Vol. 5A-2017)*. American Society of Mechanical Engineers (ASME) (2017).
<https://doi.org/10.1115/GT2017-63761>.
- [4] Sparrow, E. M., Ramsey, J. W., Altemani, C. A. C., Experiments on in-line pin fin arrays and performance comparisons with staggered arrays, *Journal of Heat Transfer*, 102(1), 44, (1980)
<https://doi.org/10.1115/1.3244247>.
- [5] Chyu, M. K., Heat transfer and pressure drop for short pin-fin arrays with pin-endwall fillet. *Journal of Heat Transfer*, 112(4), 926–932. (1990).
<https://doi.org/10.1115/1.2910502>.

- [6] Ostanek, J. K., and Thole, K. A. Effects of varying streamwise and spanwise spacing in pin-fin arrays, In Proceedings of the ASME Turbo Expo (Vol. 4, pp. 45–57), (2012).
<https://doi.org/10.1115/GT2012-68127>.
- [7] Chyu, M. K., Siw, S. C., and Moon, H. K., Effects of height-to-diameter ratio of pin element on heat transfer from staggered pin-fin arrays, In Proceedings of the ASME Turbo Expo (Vol. 3, pp. 705–713), (2009).
<https://doi.org/10.1115/GT2009-59814>.
- [8] Rao, Y., Wan, C., and Zang, S., Comparisons of flow friction and heat transfer performance in rectangular channels with pin fin-dimple, pin fin and dimple arrays, In Proceedings of the ASME Turbo Expo (Vol. 4, pp. 185–195), (2010).
<https://doi.org/10.1115/GT2010-22442>.
- [9] Rao, Y., Wan, C., Xu, Y., An experimental study of pressure loss and heat transfer in the pin fin-dimple channels with various dimple depths, International Journal of Heat and Mass Transfer, 55(23-24), 6723–6733. (2012)
<https://doi.org/10.1016/j.ijheatmasstransfer.2012.06.081>.
- [10] Rao, Y., Xu, Y., Wan, C., An experimental and numerical study of flow and heat transfer in channels with pin fin-dimple and pin fin arrays, Experimental Thermal and Fluid Science, 38, 237–247, 2012.
<https://doi.org/10.1016/j.expthermflusci.2011.12.012>.
- [11] Luo, L., Wang, C., Wang, L., Sunden, B. A., Wang, S., Heat transfer and friction factor in a dimple-pin fin wedge duct with various dimple depth and converging angle. International Journal of Numerical Methods for Heat and Fluid Flow, 26(6), 1954–1974. (2016)
<https://doi.org/10.1108/hff-02-2015-0043>.
- [12] ANSYS CFX-19.1, 2018, ANSYS Inc.
- [13] Dittus, F. W., Boelter, L. M., Heat transfer in automobile radiators of the turbulator type, University of California, Berkeley Publication, 02, 443–461, 1930.